J|A|C|S COMMUNICATIONS

Published on Web 02/11/2009

$TiO_2/TiSi_2$ Heterostructures for High-Efficiency Photoelectrochemical H_2O Splitting

Yongjing Lin, Sa Zhou, Xiaohua Liu, Stafford Sheehan, and Dunwei Wang*

Department of Chemistry, Merkert Chemistry Center, Boston College, 2609 Beacon Street, Chestnut Hill, Massachusetts 02467

Received October 27, 2008; E-mail: dunwei.wang@bc.edu

Enormous efforts have been recently focused toward seeking new materials and/or novel structures for efficient solar energy conversions.[1] Among the studied materials, TiO_2 stands out for its high incident photon-to-electron conversion efficiencies (IPCEs) and remarkable chemical stabilities.[2−5] Both photovoltaic and photoelectrochemical cells (PECs) based on TiO_2 have been investigated in recent years. Notably, Gratzel et al. have significantly advanced TiO_2-based dye-sensitized solar cells.[2] Grimes et al. have led efforts in utilizing TiO_2 nanotubes in H_2O splitting, with the potential of producing H_2 as a promising energy carrier.[3] However, implementations of TiO_2 in solar energy conversions remain limited because the performance of TiO_2-based devices is compromised by several deficiencies. For example, anatase TiO_2 has a band gap of ∼3.2 eV, confining its optical absorption in the UV range. Due to the wide band gap, as well as the low carrier densities, it is a poor conductor, limiting its capabilities in effectively collecting photogenerated electrons,[6] which becomes an increasingly important factor as charge transport plays an important role in separated H_2 and O_2 productions.[7] In addition, it lacks a complimentary p-type counterpart to complete the full H_2O splitting cycle, an issue starting to attract attention.[7] This communication aims at developing approaches to tackle these challenges using chemically synthesized heteronanostructures.

The essence of our design is schematically illustrated in Figure 1a. We combine highly conductive $TiSi_2$ nanonets (NNs) with a photoactive TiO_2 coating (Figure 1c). When in contact with the electrolyte, band bending forms at the junction and extends to the rest of the coating, yielding the depletion region.[8,9] Charges (e^- and h^+) created by incident photons are separated here. One type (e^-) is collected in the $TiSi_2$ core and readily transported away, and the other type (h^+) is transferred to the electrolyte for chemical reactions.[8] Two distinctive advantages are offered by our design: the TiO_2/electrolyte junction area is maximized, and the charge transport is improved by going through highly conductive $TiSi_2$.

The fabrication started with the growth of two-dimensional (2D) $TiSi_2$ NNs,[10] which were subsequently coated with a layer of crystalline TiO_2 in a Cambridge Nanotech Savannah atomic layer deposition (ALD) reactor (Ti(*i*-PrO)$_4$ as the precursor, Figures S1 and S2).[11] PECs were constructed and measured in 0.05 M KOH electrolyte under illuminations of a xenon lamp (150 W, Oriel Apex illuminator). The PECs consisted of three electrodes, among which $TiO_2/TiSi_2$ on Ti foil served as the working electrode and Ag/AgCl in 3 M KCl was the reference one. When measured in the dark, the current−potential plots (black trace in Figure 2a) were rectified due to the band bending at the TiO_2/solution interface. Under xenon light, a significant current (−0.6 mA/cm^2 at 0 V vs Ag/AgCl reference) was observed. The current was compensated at V_{oc} = −0.80 V. It is known that V_{oc} depends on the difference of the semiconductor flat band level and the electrochemical potential of the electrolyte.[12] We next sought to measure the conversion

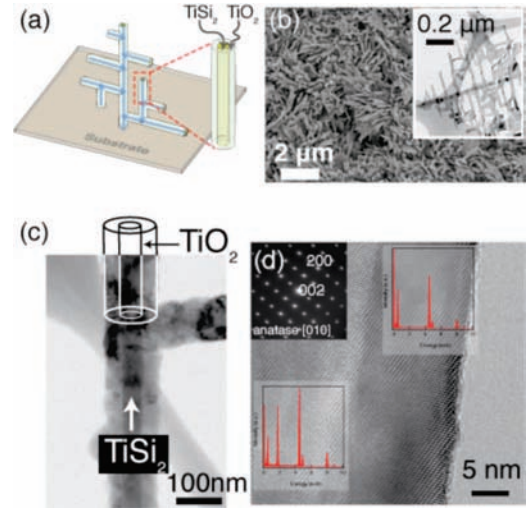

Figure 1. Structure of the $TiO_2/TiSi_2$ heterostructures. (a) A schematic sketch of the structure. Blue arrows indicate the interconnected charge transport path. (b) The scanning electron micrograph (SEM, mainframe) and the transmission electron micrograph (TEM, inset) of the nanostructures. (c) A TEM picture reveals the core/shell nature. (d) A high-resolution TEM picture shows the atomic details of the $TiO_2/TiSi_2$ interfaces. Top left inset: ED pattern confirms the anatase TiO_2 structure; EDS insets (left, $TiO_2/TiSi_2$; right, TiO_2) are different by the presence of Si.

efficiencies. It has been cautioned by Grimes et al. in ref 5 that efficiencies obtained in three-electrode configurations may lead to exaggerations due to wrong estimates of the applied voltage. We therefore borrowed the two-electrode methods and carried out the measurements. Both external quantum efficiency (or IPCE) and power conversion efficiency were measured using a 450 W xenon lamp coupled with monochromator (Jobin Yvon Flurolog3, bandpass 5 nm, see Supporting Information for details). As shown in Figure 2b, IPCE drops to 0 at incident wavelengths >385 nm,

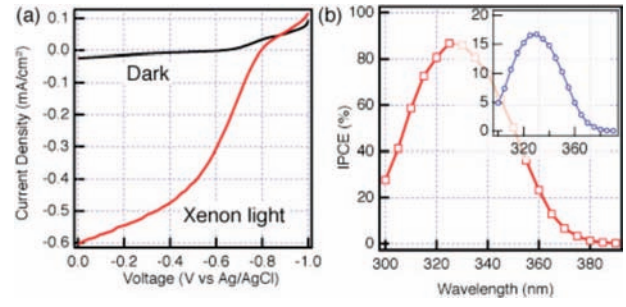

Figure 2. PEC properties of $TiO_2/TiSi_2$ heteronanostructures. (a) $I-V$ plots under different illumination conditions. (b) IPCE plots; inset: overall efficiency under monochromic illuminations (Y axis: efficiency, %; X axis: wavelength of incident light, nm).

10.1021/ja808426h CCC: $40.75

corresponding to a band gap of ~3.2 eV. The overall power conversion efficiency is presented in Figure 2b. A peak efficiency of 16.7% at ~330 nm was obtained.

In conventional semiconductor/liquid junction PECs, there is the dilemma of absorption and charge transport. A thick and lightly doped semiconductor is desired for enhanced photoabsorption and charge separation but deleterious to charge collections. TiO_2 nanotubes made by Grimes et al. represent one approach to circumvent the challenge by maximizing the TiO_2/liquid interface area and thus to fully exploit the depletion regions of TiO_2.[3] Similar improvement was achieved in our approach, as well. When compared with planar geometry, $TiO_2/TiSi_2$ exhibited a much larger photocurrent. The optimized TiO_2 coating thickness was identified as 27 nm (Supporting Information). Moreover, our strategy adds another advantage of efficient charge collections through the highly conductive $TiSi_2$ NNs. With a measured roughness factor of ~100, our devices exhibited comparable performance.

Another distinguishing feature of our approach is the deposition of TiO_2. Its versatility was next explored to tailor the properties of TiO_2, with the goal of achieving visible light absorption. As a prototypical demonstration, we chose to include W in TiO_2 to boost absorption in the visible range.[4,13] By introducing $(^tBuN)_2(Me_2N)_2W$[14] in the TiO_2 growth sequences, we successfully synthesized $W_{0.3}Ti_{0.7}O_2$ (Figure 3a, Figures S2 and S5). X-ray

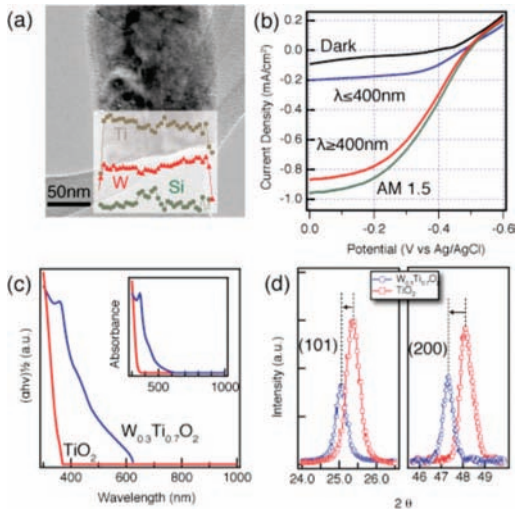

Figure 3. PEC properties of $W_{0.3}Ti_{0.7}O_2/TiSi_2$ nanostructures. (a) Microstructure and elemental analysis. (b) Current−potential plots under different illumination conditions. (c) Absorbance spectrum (inset) and optical band gap calculations. (d) X-ray diffraction patterns of anatase TiO_2 and W-TiO_2 for anatase peaks (101), left, and (200), right. The lattice constant difference is obvious (see Figure S2 for the entire pattern).

diffraction patterns confirmed the TiO_2 anatase structure. Both energy-dispersive X-ray spectroscopy (EDS) and X-ray photoelectron spectroscopy (XPS) revealed the W content in the crystalline film. As shown in Figure 3c, absorption in the visible range is significantly improved. The calculated optical band gap is reduced from 3.2 to ~2.0 eV. Corresponding PEC measurements revealed a drastically improved photocurrent in the visible range under 100 mW/cm^2 solar simulator illuminations (Oriel 96000, 150 W, equipped with AM 1.5 filters). We calculated the peak efficiency under a simulated solar light of 0.83%. We believe that the lattice distortion by the substitutition of Ti with W[15] (Figure 3d) plays an important role in the property alternations, although further systematic studies are needed to understand and optimize the system.

In conclusion, we presented a $TiO_2/TiSi_2$ core/shell heteronanostructure that was synthesized combining CVD and ALD methods. The network structure $TiSi_2$ NN provided a structural support with high surface area to improve the photon absorptions of TiO_2. Its high conductance was explored to enhance charge transport. The combined advantages led to the high performance in photoelectrochemical measurements, and a peak efficiency of 16.7% was achieved under monochromic UV illuminations. The versatility of our approach was further demonstrated by incorporating W into the TiO_2 shell to boost its visible light performance, and a peak efficiency of 0.83% was measured. A new door is opened for tackling the challenges of photosplitting H_2O using solar lights as a means to provide H_2 as a clean energy carrier.

Acknowledgment. The research is funded by Boston College. We thank Dr. T. E. Mallouk and the reviewers for their constructive comments in revising the paper. We thank Prof. P. Davidovits for his insightful discussions. Dr. D. Z. Wang assisted the XRD characterizations; S. Dimitrov helped the optical measurements; Dr. S. Lange in the Center for Nanoscale Systems (CNS, a member of the NNIN, supported by NSF: ECS-0335765) at Harvard University performed the XPS characterizations.

Supporting Information Available: Experimental details of ALD TiO_2 and $W_xTi_{1-x}O_2$ growths, photoelectrochemical measurements, efficiency calculations, roughness factor measurements, and XPS, EDS, and XRD data. This material is available free of charge via the Internet at http://pubs.acs.org.

References

(1) Lewis, N. S.; Nocera, D. G. *Proc. Natl. Acad. Sci. U.S.A.* **2006**, *103*, 15729–15735.
(2) Oregan, B.; Gratzel, M. *Nature* **1991**, *353*, 737–740.
(3) Grimes, C. A. *J. Mater. Chem.* **2007**, *17*, 1451–1457.
(4) Bak, T.; Nowotny, J.; Rekas, M.; Sorrell, C. C. *Int. J. Hydrogen Energy* **2002**, *27*, 991–1022.
(5) Varghese, O. K.; Grimes, C. A. *Sol. Energy Mater. Sol. Cells* **2008**, *92*, 374–384.
(6) Chen, X. B.; Mao, S. S. *J. Nanosci. Nanotechnol.* **2006**, *6*, 906–925.
(7) Mor, G. K.; Varghese, O. K.; Wilke, R. H. T.; Sharma, S.; Shankar, K.; Latempa, T. J.; Choi, K.-S.; Grimes, C. A. *Nano Lett.* **2008**, *8*, 1906–1911.
(8) Gratzel, M. *Nature* **2001**, *414*, 338–344.
(9) Bolton, J. R. *Solar Energy* **1996**, *57*, 37–50.
(10) Zhou, S.; Liu, X. H.; Lin, Y. J.; Wang, D. W. *Angew. Chem., Int. Ed.* **2008**, *47*, 7681–7684.
(11) Rahtu, A.; Ritala, M. *Chem. Vap. Deposition* **2002**, *8*, 21–28.
(12) Pleskov, Y. V. *Solar Energy Conversion: A Photoelectrochemical Approach*; Springer-Verlag: New York, 1990.
(13) Alexander, B. D.; Kulesza, P. J.; Rutkowska, I.; Solarska, R.; Augustynski, J. *J. Mater. Chem.* **2008**, *18*, 2298–2303. Santato, C.; Ulmann, M.; Augustynski, J. *J. Phys. Chem. B* **2001**, *105*, 936–940.
(14) Becker, J. S.; Suh, S.; Wang, S.; Gordon, R. G. *Chem. Mater.* **2003**, *15*, 2969–2976.
(15) Ghicov, A.; Yamamoto, M.; Schmuki, P. *Angew. Chem., Int. Ed.* **2008**, *47*, 7934–7937.

JA808426H